Engineering with Computers (2021) 37:3473–3488
https://doi.org/10.1007/s00366-020-01006-x

ORIGINAL ARTICLE

A local meshless method to approximate the time-fractional telegraph equation

Alpesh Kumar[1] · Akanksha Bhardwaj[1] · Shruti Dubey[2]

Received: 22 January 2020 / Accepted: 11 March 2020 / Published online: 23 March 2020
© Springer-Verlag London Ltd., part of Springer Nature 2020

Abstract
In the present work, we investigate the numerical solution of time-fractional telegraph equation by a local meshless method. The fractional-order derivative is defined in the Caputo's sense. The time semi-discretization was carried out using finite difference method followed by radial basis function-based spatial discretization. The theoretical convergence analysis and stability analysis of time semi-discrete scheme are also proved. Several test problems with regular and irregular domains with uniform and non-uniform points are considered. To demonstrate the accuracy and efficiency of the proposed method, we compared the analytical and numerical solution of the proposed problem.

Keywords Radial basis function · Local collocation method · Finite difference · Time fractional · Telegraph equation

1 Introduction

In recent decades, fractional calculus has become a powerful tool because many complex problems can be easily and successfully modeled in various fields by fractional calculus. Fractional calculus has many applications in the fields of science, engineering, and finance [2, 4, 6, 8, 24, 48, 57]. Fractional partial differential equations are obtained by replacing integer-order derivatives of partial differential equations with fractional-order derivatives. A lot of publications related to fractional partial differential equations are presented; for example, see [10, 19, 47, 52, 62, 64].

In this paper, we are dealing with following time-fractional telegraph equation

$$\begin{cases} {}_0^c\mathscr{D}_t^{\alpha} u(\mathbf{x},t) + {}_0^c\mathscr{D}_t^{\alpha-1} u(\mathbf{x},t) + u(\mathbf{x},t) = \Delta u(\mathbf{x},t) + f(\mathbf{x},t), & (\mathbf{x},t) \in \Omega \times (0,T], \\ u(\mathbf{x},0) = \xi(\mathbf{x}), \quad \frac{\partial u(\mathbf{x},0)}{\partial t} = \psi(\mathbf{x}), & \mathbf{x} \in \Omega \\ u(\mathbf{x},t) = \zeta(\mathbf{x},t), & \mathbf{x} \in \partial\Omega, \end{cases} \tag{1.1}$$

where $1 < \alpha < 2$, $T > 0$ and $\xi(\mathbf{x})$, $\psi(\mathbf{x})$, $\zeta(\mathbf{x},t)$ and $f(\mathbf{x},t)$ are sufficiently smooth functions on closed and bounded domain $\Omega \subset \mathbb{R}^2$, with boundary $\partial\Omega$. Moreover, for any given positive integer, the Caputo's differential operator k, ${}_0^c\mathscr{D}_t^{\alpha} u(\mathbf{x},t)$ is defined as

$${}_0^c\mathscr{D}_t^{\alpha} u(\mathbf{x},t) = \begin{cases} \frac{1}{\Gamma(k-\alpha)} \int\limits_0^t \frac{\partial^k u(\mathbf{x},s)}{\partial s^k} \frac{\mathrm{d}s}{(t-s)^{\alpha-(k-1)}}, & k-1 < \alpha < k, \\ \frac{\partial^k u(\mathbf{x},t)}{\partial t^k}, & \alpha = k. \end{cases} \tag{1.2}$$

It is found that the classical telegraph equation has many applications in neutron transport [59], random walk of

✉ Akanksha Bhardwaj
pmth17001@rgipt.ac.in; bhardwaj.ak11@gmail.com

Alpesh Kumar
alpeshk@rgipt.ac.in; alpeshmath@gmail.com

Shruti Dubey
sdubey@iitm.ac.in

[1] Department of Basic Sciences and Humanities, Rajiv Gandhi Institute of Petroleum Technology, Jais, Amethi, India

[2] Department of Mathematics, Indian Institute of Technology Madras, Chennai, India

suspension flows [3], signal analysis, propagation and transmission of electrical signals [36], etc. Recently, fractional telegraph equation has been solved by many authors. Mittal and Bhatia [37] developed differential quadrature method based on cubic B-spline basis function to solve hyperbolic telegraph equation. Ömer Oruç [41] considered two-dimensional hyperbolic telegraph equation using finite difference method in time and Hermite wavelets approach for space. In [28] Jiang and Lin solved time-fractional telegraph equation using reproducing kernel theorem. Kumar et al. [31] considered a generalized time-fractional telegraph-type equation using a numerical scheme based on the finite difference method. Liang et al. [33] discussed time-fractional telegraph equation using a fast high-order difference scheme. In [17] Dehghan et al. solved four different types of linear telegraph equations using He's variational iteration method. Li and Cao [32] used finite difference method to solve linear time-fractional telegraph equation. In [39] Adomian decomposition method is derived by Momani to solve space- and time-fractional telegraph equation. Chen et al. [5] derived the analytical solution of time-fractional telegraph equation and applied the method of separating variables. Yildirim [61] proposed homotopy perturbation method (HPM) to solve space- and time-fractional telegraph equation. Wang and Mei [60] presented the time-fractional telegraph equation using a generalized finite difference method in time and Legendre spectral Galerkin method in space. In [7] homotopy analysis method (HAM) is presented by Das et al. to solve the time-fractional telegraph equation. A finite difference method in time and Galerkin finite element method in space are used to solve the time–space-fractional telegraph equation by Zhao and Li [63].

Recently, radial basis function (RBF)-based meshfree methods are increasingly attracted the attention of the researchers for solving fractional partial differential equations. Several problems [6, 12, 18, 27, 35, 46, 54] of fractional partial differential equations have been solved by many researchers and references therein. Abbaszadeh and Dehghan [1] considered the distributed order time-fractional diffusion-wave equation using interpolating element-free Galerkin method. Recently, Kumar et al. [29, 30] considered time-fractional linear and nonlinear diffusion-wave equation using RBF-based meshless local collocation method, respectively. For further applications of meshless methods, we refer Nikan et al. [40], Dehghan et al. [9, 11, 13, 15], Ghehsareh et al. [20–23], Liu et al. [34], Salehi et al. [49] Shivanian and Jafarabadi [54, 55] and references therein. Recently, Oruç [45] developed two meshless methods, in which one is based on local radial basis function and other is based on barycentric rational interpolation for solving 2D viscoelastic wave equation, and also the same author in [42–44] proposed a meshless method based on multiple-scale Pascal polynomials for different problems. This method is easily implemented for the problems of irregular domain as it is mesh independent. Hosseini et al. in [25, 26] developed radial basis function-based method and meshless local radial point interpolation (MLRPI) method to solve time-fractional telegraph equation, respectively. Shivanian [51] considered a time-fractional telegraph equation using spectral meshless radial point interpolation (SMRPI) method. In [14] a meshless local weak-strong (MLWS) method is derived by Dehghan and Ghesmati to solve a hyperbolic telegraph equation. In [16] a hyperbolic telegraph equation is solved using RBF collocation method by Dehghan and Shokri. The nonlinear time-fractional telegraph equation is solved by Sepehrian and Shamohammadi [50] with collocation method. Mohebbi et al. [38] proposed a RBF-based meshless method to solve time-fractional telegraph equation. Shivanian et al. [56] solved telegraph equation using meshless local radial point interpolation (MLRPI) method. Shivanian et al. [53] considered a time-fractional telegraph equation using meshless local Petrov–Galerkin (MLPG) method in which Galerkin weak form and moving least-squares (MLS) approximation is applied.

This manuscript is organized as follows: Time semi-discretization scheme is described in Sect. 2; furthermore, in this section stability and convergence analysis of the time discrete numerical scheme is also described. In Sect.3, we have briefly discussed the local collocation method and how the proposed method is numerically implemented. We examined some numerical experiments to demonstrate the computational efficiency and accuracy of the proposed method in Sect. 4. In Sect. 5, we end this paper finally, with the help of some concluding remark.

2 The time semi-discretization

In the present section, we will develop and analyze the time semi-discrete scheme of the proposed Eq. (1.1), and the Caputo's fractional derivative ${}_0^c\mathscr{D}_t^\alpha u(\mathbf{x},t)$ could be rewritten as follows

$$
{}_0^c\mathscr{D}_t^\alpha u(\mathbf{x},t) = \begin{cases} \frac{1}{\Gamma(1-\alpha)} \int\limits_0^t \frac{\partial u(\mathbf{x},s)}{\partial s} \frac{\mathrm{d}s}{(t-s)^\alpha}, & 0<\alpha<1, \\ \frac{1}{\Gamma(2-\alpha)} \int\limits_0^t \frac{\partial^2 u(\mathbf{x},s)}{\partial s^2} \frac{\mathrm{d}s}{(t-s)^{\alpha-1}}, & 1<\alpha<2. \end{cases} \tag{2.1}
$$

If $1<\alpha<2$, then $0<\alpha-1<1$, so

$$
\begin{aligned} {}_0^c\mathscr{D}_t^{\alpha-1} u(\mathbf{x},t) =& \frac{1}{\Gamma(1-(\alpha-1))} \int\limits_0^t \frac{\partial u(\mathbf{x},s)}{\partial s} \frac{\mathrm{d}s}{(t-s)^{\alpha-1}} \\ =& \frac{1}{\Gamma(2-\alpha)} \int\limits_0^t \frac{\partial u(\mathbf{x},s)}{\partial s} \frac{\mathrm{d}s}{(t-s)^{\alpha-1}}. \end{aligned} \tag{2.2}
$$

For any positive integer N, we let $\delta t = \frac{T}{N}$, be the step size in time, and $t_n = n\delta t,\ n \in \mathbb{N}^+$ are the temporal discretization points. Now, we define the notation as $u^{n-\frac{1}{2}} = \frac{1}{2}(u^n + u^{n-1})$, and $\delta_t u^{n-\frac{1}{2}} = \frac{1}{\delta t}(u^n - u^{n-1})$, together with u^n being the abbreviation of the $u(\mathbf{x}, t_n)$.

Lemma 1 *Let us suppose $\eta(t) \in C^2[0,T]$ and $1 < \alpha < 2$, it holds that*

$$\int_0^{t_n} \eta'(s)(t_n - s)^{1-\alpha}\mathrm{d}s = \sum_{k=1}^{n} \frac{\eta(t_k) - \eta(t_{k-1})}{\delta t} \int_{t_{k-1}}^{t_k} (t_n - s)^{1-\alpha}\mathrm{d}s + R^n,\ 1 \le n \le N \tag{2.3}$$

and

$$|R^n| \le \left(\frac{1}{2(2-\alpha)} + \frac{1}{2}\right)\delta t^{3-\alpha} \max_{0\le t\le t_n} |\eta''(t)|. \tag{2.4}$$

Proof See Sun et al. [58]. □

Lemma 2 *Let* $1 < \alpha < 2$, $a_0 = \frac{1}{\delta t\Gamma(2-\alpha)}$ *and* $b_k = \frac{\delta t^{2-\alpha}}{(2-\alpha)}\left[(k+1)^{2-\alpha} - (k)^{2-\alpha}\right]$, *then*

$$\left|\frac{1}{\Gamma(2-\alpha)}\int_0^{t_n} \frac{\eta'(s)}{(t_n - s)^{\alpha-1}}\mathrm{d}s - a_0\left[b_0\eta(t_n) - \sum_{k=1}^{n-1}(b_{n-k-1} - b_{n-k})\eta(t_k) - b_{n-1}\eta(0)\right]\right| \le \frac{1}{2\Gamma(2-\alpha)}\left(1 + \frac{1}{(2-\alpha)}\right)\delta t^{3-\alpha} \max_{0\le t\le t_n} |\eta''(t)| \tag{2.5}$$

Proof Directly follows from Lemma 1. □

Lemma 3 *Let* $b_k = \frac{\delta t^{2-\alpha}}{(2-\alpha)}\left[(k+1)^{2-\alpha} - (k)^{2-\alpha}\right]$, *where* $1 < \alpha < 2$, $k = 0, 1, 2, \ldots$, *then*

$b_0 > b_1 > b_2 > \ldots > b_k \to 0$, as $k \to \infty$.

Proof See Sun et al. [58]. □

For convention of the theory let us define,

$$v(\mathbf{x}, t) = \frac{\partial u(\mathbf{x}, t)}{\partial t} \tag{2.6}$$

$$w(\mathbf{x}, t) = \frac{1}{\Gamma(2-\alpha)}\int_0^t \frac{\partial v(\mathbf{x}, s)}{\partial s}\frac{\mathrm{d}s}{(t-s)^{\alpha-1}} \tag{2.7}$$

$$z(\mathbf{x}, t) = \frac{1}{\Gamma(2-\alpha)}\int_0^t \frac{\partial u(\mathbf{x}, s)}{\partial s}\frac{\mathrm{d}s}{(t-s)^{\alpha-1}} \tag{2.8}$$

Now applying Taylor expansion on (2.6), we have

$$v^{n-\frac{1}{2}} = \delta_t u^{n-\frac{1}{2}} + r_1^{n-\frac{1}{2}} \tag{2.9}$$

and the numerical scheme is

$$\begin{aligned} &w^{n-\frac{1}{2}} + z^{n-\frac{1}{2}} + u^{n-\frac{1}{2}} \\ &\quad = \Delta u^{n-\frac{1}{2}} + f^{n-\frac{1}{2}} + r_2^{n-\frac{1}{2}},\quad n \ge 1, \end{aligned} \tag{2.10}$$

where $r_1^{n-\frac{1}{2}}$ and $r_2^{n-\frac{1}{2}}$ are the local truncation errors which is bounded by

$$|r_1^{n-\frac{1}{2}}| \le C_1\delta t^2, \quad |r_2^{n-\frac{1}{2}}| \le C_2\delta t^2. \tag{2.11}$$

Discretizing Eqs. (2.7) and (2.8), we have

$$w(\mathbf{x}, t_n) = \frac{1}{\Gamma(2-\alpha)}\int_0^{t_n} \frac{\partial v(\mathbf{x}, t)}{\partial t}\frac{\mathrm{d}t}{(t_n - t)^{\alpha-1}}$$

$$z(\mathbf{x}, t_n) = \frac{1}{\Gamma(2-\alpha)}\int_0^{t_n} \frac{\partial u(\mathbf{x}, t)}{\partial t}\frac{\mathrm{d}t}{(t_n - t)^{\alpha-1}},$$

using Lemma 2, we have

$$\begin{aligned} w^n = &a_0\left[b_0 v^n - \sum_{k=1}^{n-1}(b_{n-k-1} - b_{n-k})v^k - b_{n-1}v^0\right] \\ &+ \mathcal{O}(\delta t^{3-\alpha}), \end{aligned} \tag{2.12}$$

$$\begin{aligned} z^n = &a_0\left[b_0 u^n - \sum_{k=1}^{n-1}(b_{n-k-1} - b_{n-k})u^k - b_{n-1}u^0\right] \\ &+ \mathcal{O}(\delta t^{3-\alpha}). \end{aligned} \tag{2.13}$$

Now define the operator [58]

$$\mathcal{P}(v^n, q) = \left[b_0 v^n - \sum_{k=1}^{n-1}(b_{n-k-1} - b_{n-k})v^k - b_{n-1}q\right],$$

and using both the initial condition $v^0 = v(\mathbf{x}, 0) = \psi$ and $u^0 = u(\mathbf{x}, 0) = \xi$, we have

$$w^{n-\frac{1}{2}} = a_0\mathcal{P}(v^{n-\frac{1}{2}}, \psi) + \left(r_3\right)^{n-\frac{1}{2}}, \tag{2.14}$$

$$z^{n-\frac{1}{2}} = a_0\mathcal{P}(u^{n-\frac{1}{2}}, \xi) + \left(r_4\right)^{n-\frac{1}{2}}, \tag{2.15}$$

where

$$|(r_3)^{n-\frac{1}{2}}| \leq C_3\delta t^{3-\alpha} \text{ and } |(r_4)^{n-\frac{1}{2}}| \leq C_4\delta t^{3-\alpha} \tag{2.16}$$

Now substituting (2.9) into (2.15), we have

$$w^{n-\frac{1}{2}} = a_0\mathcal{P}(\delta_t u^{n-\frac{1}{2}},\psi) + a_0\mathcal{P}(r_1^{n-\frac{1}{2}},0) + (r_3)^{n-\frac{1}{2}}, \tag{2.17}$$

now substituting (2.15) and above expression in (2.10), we have

$$\begin{aligned} a_0\mathcal{P}(\delta_t u^{n-\frac{1}{2}},\psi) &+ a_0\mathcal{P}(r_1^{n-\frac{1}{2}},0) \\ &+ r_3^{n-\frac{1}{2}} + a_0\mathcal{P}(u^{n-\frac{1}{2}},\xi) + r_4^{n-\frac{1}{2}} = \Delta u^{n-\frac{1}{2}} + f^{n-\frac{1}{2}} \\ &+ r_2^{n-\frac{1}{2}} \\ a_0\mathcal{P}(\delta_t u^{n-\frac{1}{2}},\psi) &+ a_0\mathcal{P}(u^{n-\frac{1}{2}},\xi) \\ &= \Delta u^{n-\frac{1}{2}} + f^{n-\frac{1}{2}} + R^{n-\frac{1}{2}} \end{aligned} \tag{2.18}$$

where

$$\begin{aligned} R^{n-\frac{1}{2}} &= -\left\{ a_0\mathcal{P}(r_1^{n-\frac{1}{2}},0) + r_3^{n-\frac{1}{2}} + r_4^{n-\frac{1}{2}} \right\} + r_2^{n-\frac{1}{2}} \\ |R^{n-\frac{1}{2}}| &= \left| -\left\{ a_0\mathcal{P}(r_1^{n-\frac{1}{2}},0) + r_3^{n-\frac{1}{2}} + r_4^{n-\frac{1}{2}} \right\} + r_2^{n-\frac{1}{2}} \right| \\ &\leq \Bigg\{ a_0\left[b_0 r_1^{n-\frac{1}{2}} + \sum_{k=1}^{n-1}(b_{n-k-1}-b_{n-k})r_1^{k-\frac{1}{2}} \right] \\ &\quad + r_3^{n-\frac{1}{2}} + r_4^{n-\frac{1}{2}} \Bigg\} + r_2^{n-\frac{1}{2}} \\ &\leq \Bigg\{ a_0\left[b_0 C_1\delta t^2 + \sum_{k=1}^{n-1}(b_{n-k-1}-b_{n-k})C_1\delta t^2 \right] \\ &\quad + C_3\delta t^{3-\alpha} + C_4\delta t^{3-\alpha} \Bigg\} + C_2\delta t^2 \\ &= \left\{ a_0\left[b_0 C_1\delta t^2 + (b_0-b_{n-1})C_1\delta t^2 \right] \right. \\ &\quad \left. + C_3\delta t^{3-\alpha} + C_4\delta t^{3-\alpha} \right\} + C_2\delta t^2 \\ &\leq \left\{ a_0\left[2b_0 C_1\delta t^2 \right] \right. \\ &\quad \left. + C_3\delta t^{3-\alpha} + C_4\delta t^{3-\alpha} \right\} + C_2\delta t^2 \\ &= \Bigg\{ \frac{1}{\delta t\Gamma(2-\alpha)}\left[\frac{2\delta t^{2-\alpha}C_1\delta t^2}{(2-\alpha)} \right] \\ &\quad + C_3\delta t^{3-\alpha} + C_4\delta t^{3-\alpha} \Bigg\} + C_2\delta t^2 \\ &\leq C\delta t^{3-\alpha}. \end{aligned}$$

where $C = \left\{ \left[\frac{2C_1}{(2-\alpha)\Gamma(2-\alpha)} + C_3 + C_4 \right] + C_2 \right\}$. Now omitting the truncation error term $R^{n-\frac{1}{2}}$ from Eq. (2.18), with exact value u^n is approximated by its numerical approximation U^n, The resulted numerical scheme is as follows:

$$\begin{aligned} a_0\mathcal{P}(\delta_t U^{n-\frac{1}{2}} &+ U^{n-\frac{1}{2}},\psi+\xi) + U^{n-\frac{1}{2}} \\ &= \Delta U^{n-\frac{1}{2}} + f^{n-\frac{1}{2}}, \quad 1 \leq n \leq N. \end{aligned} \tag{2.19}$$

The above equation can be written in more precise form as

$$\mathcal{L}U^n = F, \tag{2.20}$$

where $\mathcal{L}$ and F are given as:

$$\begin{cases} \mathcal{L}U^n &= \frac{1}{\delta t\Gamma(2-\alpha)}\frac{b_0}{\delta t}U^n + \frac{1}{\delta t\Gamma(2-\alpha)}\frac{b_0}{2}U^n + \frac{1}{2}U^n - \frac{1}{2}\Delta U^n \\ F &= \frac{1}{\delta t\Gamma(2-\alpha)}\frac{b_0}{\delta t}U^{n-1} - \frac{1}{\delta t\Gamma(2-\alpha)}\frac{b_0}{2}U^{n-1} - \frac{1}{2}U^{n-1} + \frac{1}{2}\Delta U^{n-1} + \\ & \frac{1}{\delta t\Gamma(2-\alpha)}\sum_{k=1}^{n-1}(b_{n-k-1}-b_{n-k})(\delta_t U^{k-\frac{1}{2}} + U^{k-\frac{1}{2}}) + \frac{1}{\delta t\Gamma(2-\alpha)}b_{n-1}(\psi+\xi) \\ & + f^{n-\frac{1}{2}}. \end{cases}$$

2.1 Convergence and stability analysis

This section devoted to discuss the stability of the time semi-discrete scheme and also to prove that the time discrete scheme is convergent with convergence order $\delta t^{3-\alpha}$ in L_2 norm.

Lemma 4 *For any function $\eta = \{\eta_1,\eta_2,\dots\}$, θ with $1 < \alpha < 2$, we have*

$$\sum_{i=1}^{n}\mathcal{P}(\eta_i,\theta)\eta_i \geq \frac{t_n^{1-\alpha}}{2}\delta t\sum_{i=1}^{n}\eta_i^2 - \frac{t_n^{2-\alpha}}{2(2-\alpha)}\theta^2$$

Proof See [58]. □

As the considered problem (1.1) is linear, it is sufficient to do analysis for homogeneous boundary conditions, i.e., $\zeta(\mathbf{x},t) = 0$.

Theorem 1 *Let $U^n \in H_0^1$, the time discrete scheme (2.19) is unconditionally stable and we have the following inequality:*

$$\|U^n\|^2 \leq C\left(\|\xi\|^2 + \|\nabla\xi\|^2 + \|\psi+\xi\|^2 + \max_{1\leq j\leq n}\|f^{j-\frac{1}{2}}\|^2 \right).$$

Proof Multiplying Eq. (2.19) by $(\delta_t U^{n-\frac{1}{2}} + U^{n-\frac{1}{2}})$ and integrating over Ω give

$$\begin{aligned} a_0\Big\{ b_0\Big(\delta_t U^{n-\frac{1}{2}} &+ U^{n-\frac{1}{2}}, \delta_t U^{n-\frac{1}{2}} + U^{n-\frac{1}{2}}\Big) \\ &- \sum_{k=1}^{n-1}(b_{n-k-1}-b_{n-k})\Big(\delta_t U^{k-\frac{1}{2}} + U^{k-\frac{1}{2}}, \delta_t U^{n-\frac{1}{2}} + U^{n-\frac{1}{2}}\Big) \\ &- b_{n-1}\Big(\psi+\xi, \delta_t U^{n-\frac{1}{2}} + U^{n-\frac{1}{2}}\Big)\Big\} + \Big(U^{n-\frac{1}{2}}, \delta_t U^{n-\frac{1}{2}} + U^{n-\frac{1}{2}}\Big) \\ &= \Big(\Delta U^{n-\frac{1}{2}}, \delta_t U^{n-\frac{1}{2}} + U^{n-\frac{1}{2}}\Big) + \Big(f^{n-\frac{1}{2}}, \delta_t U^{n-\frac{1}{2}} + U^{n-\frac{1}{2}}\Big), \end{aligned} \tag{2.21}$$

where $(\cdot,\cdot)$ is used for inner product. Now we are using the following fact

$$
\begin{aligned}
&\left(U^{n-\frac{1}{2}}, \delta_t U^{n-\frac{1}{2}} + U^{n-\frac{1}{2}}\right) \\
&= \left(U^{n-\frac{1}{2}}, \delta_t U^{n-\frac{1}{2}}\right) + \left(U^{n-\frac{1}{2}}, U^{n-\frac{1}{2}}\right) \\
&= \int_\Omega \left(\frac{U^n + U^{n-1}}{2}\right)\left(\frac{U^n - U^{n-1}}{\delta t}\right) \mathrm{d}\Omega + \int_\Omega \left(U^{n-\frac{1}{2}}\right)^2 \mathrm{d}\Omega \\
&= \frac{1}{2\delta t} \int_\Omega \left[(U^n)^2 - (U^{n-1})^2\right] \mathrm{d}\Omega + \int_\Omega \left(U^{n-\frac{1}{2}}\right)^2 \mathrm{d}\Omega \\
&= \frac{1}{2\delta t}\left(\|U^n\|^2 - \|U^{n-1}\|^2\right) + \|U^{n-\frac{1}{2}}\|^2
\end{aligned}
$$

and

$$
\begin{aligned}
&\left(\Delta U^{n-\frac{1}{2}}, \delta_t U^{n-\frac{1}{2}} + U^{n-\frac{1}{2}}\right) \\
&= -\left(\nabla U^{n-\frac{1}{2}}, \nabla\left(\delta_t U^{n-\frac{1}{2}} + U^{n-\frac{1}{2}}\right)\right) \\
&= -\left(\nabla U^{n-\frac{1}{2}}, \nabla \delta_t U^{n-\frac{1}{2}} + \nabla U^{n-\frac{1}{2}}\right) \\
&= -\left[\left(\nabla U^{n-\frac{1}{2}}, \nabla \delta_t U^{n-\frac{1}{2}}\right) + \left(\nabla U^{n-\frac{1}{2}}, \nabla U^{n-\frac{1}{2}}\right)\right] \\
&= -\int_\Omega \left(\frac{\nabla U^n + \nabla U^{n-1}}{2}\right)\left(\frac{\nabla U^n - \nabla U^{n-1}}{\delta t}\right) \mathrm{d}\Omega \\
&\quad - \int_\Omega \left(\nabla U^{n-\frac{1}{2}}\right)^2 \mathrm{d}\Omega \\
&= -\frac{1}{2\delta t} \int_\Omega \left[(\nabla U^n)^2 - (\nabla U^{n-1})^2\right] \mathrm{d}\Omega - \int_\Omega \left(\nabla U^{n-\frac{1}{2}}\right)^2 \mathrm{d}\Omega \\
&= -\frac{1}{2\delta t}\left(\|\nabla U^n\|^2 - \|\nabla U^{n-1}\|^2\right) - \|\nabla U^{n-\frac{1}{2}}\|^2
\end{aligned}
$$

we have

$$
\begin{aligned}
&a_0 \Big\{ b_0 \|\delta_t U^{n-\frac{1}{2}} + U^{n-\frac{1}{2}}\|^2 \\
&\quad - \sum_{k=1}^{n-1} \left(b_{n-k-1} - b_{n-k}\right) \|\delta_t U^{k-\frac{1}{2}} \\
&\quad + U^{k-\frac{1}{2}}\| \|\delta_t U^{n-\frac{1}{2}} + U^{n-\frac{1}{2}}\| \\
&\quad - b_{n-1} \|\psi + \xi\| \|\delta_t U^{n-\frac{1}{2}} + U^{n-\frac{1}{2}}\| \Big\} \\
&\quad + \frac{1}{2\delta t}\left(\|U^n\|^2 - \|U^{n-1}\|^2\right) + \|U^{n-\frac{1}{2}}\|^2 \\
&\leq -\|\nabla U^{n-\frac{1}{2}}\|^2 - \frac{1}{2\delta t}\left(\|\nabla U^n\|^2 - \|\nabla U^{n-1}\|^2\right) \\
&\quad + \|f^{n-\frac{1}{2}}\| \|\delta_t U^{n-\frac{1}{2}} + U^{n-\frac{1}{2}}\|;
\end{aligned}
$$

now taking the summation from $n = 1$ to $n = m$ on both sides of the above inequality, we have

$$
\begin{aligned}
&a_0 \sum_{n=1}^{m} \Big\{ b_0 \|\delta_t U^{n-\frac{1}{2}} + U^{n-\frac{1}{2}}\| \\
&\quad - \sum_{k=1}^{n-1} \left(b_{n-k-1} - b_{n-k}\right) \|\delta_t U^{k-\frac{1}{2}} \\
&\quad + U^{k-\frac{1}{2}}\| - b_{n-1} \|\psi + \xi\| \Big\} \|\delta_t U^{n-\frac{1}{2}} + U^{n-\frac{1}{2}}\| \\
&\quad + \frac{1}{2\delta t}\left(\|U^m\|^2 - \|U^0\|^2\right) + \sum_{n=1}^{m} \|U^{n-\frac{1}{2}}\|^2 \\
&\leq -\frac{1}{2\delta t}\left(\|\nabla U^m\|^2 - \|\nabla U^0\|^2\right) - \sum_{n=1}^{m} \|\nabla U^{n-\frac{1}{2}}\|^2 \\
&\quad + \sum_{n=1}^{m} \|f^{n-\frac{1}{2}}\| \|\delta_t U^{n-\frac{1}{2}} + U^{n-\frac{1}{2}}\|.
\end{aligned}
\tag{2.22}
$$

Also using inequality $|xy| \leq \frac{1}{2\theta}x^2 + \frac{\theta}{2}y^2$, together with $\theta = \frac{t_m^{1-\alpha}}{\Gamma(2-\alpha)}$, we get

$$
\begin{aligned}
&\sum_{n=1}^{m} \|f^{n-\frac{1}{2}}\| \|\delta_t U^{n-\frac{1}{2}} + U^{n-\frac{1}{2}}\| \\
&\leq \frac{\Gamma(2-\alpha)}{2t_m^{1-\alpha}} \sum_{n=1}^{m} \|f^{n-\frac{1}{2}}\|^2 \\
&\quad + \frac{t_m^{1-\alpha}}{2\Gamma(2-\alpha)} \sum_{n=1}^{m} \|\delta_t U^{n-\frac{1}{2}} + U^{n-\frac{1}{2}}\|^2.
\end{aligned}
$$

Now using above relation together with Lemma 4, we have

$$
\begin{aligned}
&\frac{t_m^{1-\alpha}}{2\delta t \Gamma(2-\alpha)} \delta t \sum_{n=1}^{m} \|\delta_t U^{n-\frac{1}{2}} + U^{n-\frac{1}{2}}\|^2 \\
&\quad - \frac{t_m^{2-\alpha}}{2\delta t \Gamma(3-\alpha)} \|\psi + \xi\|^2 + \frac{1}{2\delta t}\left(\|U^m\|^2 - \|U^0\|^2\right) \\
&\quad + \sum_{n=1}^{m} \|U^{n-\frac{1}{2}}\|^2 \\
&\leq -\frac{1}{2\delta t}\left(\|\nabla U^m\|^2 - \|\nabla U^0\|^2\right) - \sum_{n=1}^{m} \|\nabla U^{n-\frac{1}{2}}\|^2 \\
&\quad + \frac{\Gamma(2-\alpha)}{2t_m^{1-\alpha}} \sum_{n=1}^{m} \|f^{n-\frac{1}{2}}\|^2 + \frac{t_m^{1-\alpha}}{2\Gamma(2-\alpha)} \sum_{n=1}^{m} \|\delta_t U^{n-\frac{1}{2}} + U^{n-\frac{1}{2}}\|^2.
\end{aligned}
$$

Now simplifying above relation and switching index from m to n, we have

$$
\begin{aligned}
&\|U^n\|^2 + \|\nabla U^n\|^2 + 2\delta t \sum_{k=1}^{n} \|U^{k-\frac{1}{2}}\|^2 + 2\delta t \sum_{k=1}^{n} \|\nabla U^{k-\frac{1}{2}}\|^2 \\
&\leq \left(\|U^0\|^2 + \|\nabla U^0\|^2\right) + \frac{t_n^{2-\alpha}}{\Gamma(3-\alpha)} \|\psi + \xi\|^2 \\
&\quad + \Gamma(2-\alpha) t_n^{\alpha-1} \delta t \sum_{j=1}^{n} \|f^{j-\frac{1}{2}}\|^2,
\end{aligned}
\tag{2.23}
$$

$$\|U^n\|^2 \leq \left(\|\nabla U^0\|^2 + \|U^0\|^2\right) + \frac{t_n^{2-\alpha}}{\Gamma(3-\alpha)}\|\psi + \xi\|^2 + \Gamma(2-\alpha)t_n^{\alpha-1} n\delta t \max_{1\leq j\leq n}\|f^{j-\frac{1}{2}}\|^2, \tag{2.24}$$

$$\begin{aligned}\|U^n\|^2 &\leq \left(\|\nabla U^0\|^2 + \|U^0\|^2\right) + \frac{T^{2-\alpha}}{\Gamma(3-\alpha)}\|\psi + \xi\|^2 + \Gamma(2-\alpha)T^{\alpha} \max_{1\leq j\leq n}\|f^{j-\frac{1}{2}}\|^2, \\ &= \left(\|\nabla \xi\|^2 + \|\xi\|^2\right) + \frac{T^{2-\alpha}}{\Gamma(3-\alpha)}\|\psi + \xi\|^2 + \Gamma(2-\alpha)T^{\alpha} \max_{1\leq j\leq n}\|f^{j-\frac{1}{2}}\|^2,\end{aligned} \tag{2.25}$$

where $\psi = U_t^0$ and $\xi = U^0$. Therefore, we have

$$\|U^n\|^2 \leq C\left(\|\nabla \xi\|^2 + \|\xi\|^2 + \|\psi + \xi\|^2 + \max_{1\leq j\leq n}\|f^{j-\frac{1}{2}}\|^2\right),$$

where $C = \left(1 + \frac{T^{2-\alpha}}{\Gamma(3-\alpha)} + T^{\alpha}\Gamma(2-\alpha)\right)$. □

Theorem 2 *Let u^n and U^n both belonging to H^1 be the analytical and numerical solution of (2.18) and (2.19), respectively, then time semi-discrete scheme defined by (2.19) have $\mathcal{O}(\delta t^{3-\alpha})$ convergence order .*

Proof Let us define $\mathcal{E}^n = u^n - U^n$ with $n \geq 1$, and also $\mathcal{E}^0 = 0$. From Eqs. (2.18) and (2.19), we get

$$\begin{aligned}&a_0\left\{b_0\left(\delta_t\mathcal{E}^{n-\frac{1}{2}} + \mathcal{E}^{n-\frac{1}{2}}\right) - \sum_{k=1}^{n-1}(b_{n-k-1} - b_{n-k})\left(\delta_t\mathcal{E}^{k-\frac{1}{2}} + \mathcal{E}^{k-\frac{1}{2}}\right)\right\} + \mathcal{E}^{n-\frac{1}{2}} \\ &= \Delta\mathcal{E}^{n-\frac{1}{2}} + R^{n-\frac{1}{2}},\end{aligned} \tag{2.26}$$

Multiplying the above equation by $(\delta_t\mathcal{E}^{n-\frac{1}{2}} + \mathcal{E}^{n-\frac{1}{2}})$, and integrating over Ω, gives

$$\begin{aligned}&a_0\left\{b_0\|\delta_t\mathcal{E}^{n-\frac{1}{2}} + \mathcal{E}^{n-\frac{1}{2}}\| - \sum_{k=1}^{n-1}(b_{n-k-1} - b_{n-k})\|\delta_t\mathcal{E}^{k-\frac{1}{2}} + \mathcal{E}^{k-\frac{1}{2}}\|\right\} \\ &\|\delta_t\mathcal{E}^{n-\frac{1}{2}} + \mathcal{E}^{n-\frac{1}{2}}\| + \frac{1}{2\delta t}\left(\|\mathcal{E}^n\|^2 - \|\mathcal{E}^{n-1}\|^2\right) + \|\mathcal{E}^{n-\frac{1}{2}}\|^2 \\ &= -\frac{1}{2\delta t}\left(\|\nabla\mathcal{E}^n\|^2 - \|\nabla\mathcal{E}^{n-1}\|^2\right) - \|\nabla\mathcal{E}^{n-\frac{1}{2}}\|^2 + (R^{n-\frac{1}{2}}, \delta_t\mathcal{E}^{n-\frac{1}{2}} + \mathcal{E}^{n-\frac{1}{2}})\end{aligned}$$

Now summing the above relation from $n = 1$ to m, we have

$$\begin{aligned}&\sum_{n=1}^{m}\frac{1}{\delta t\Gamma(2-\alpha)}\left\{b_0\|\delta_t\mathcal{E}^{n-\frac{1}{2}} + \mathcal{E}^{n-\frac{1}{2}}\| - \sum_{k=1}^{n-1}(b_{n-k-1} - b_{n-k})\|\delta_t\mathcal{E}^{k-\frac{1}{2}} + \mathcal{E}^{k-\frac{1}{2}}\|\right\} \\ &\|\delta_t\mathcal{E}^{n-\frac{1}{2}} + \mathcal{E}^{n-\frac{1}{2}}\| + \frac{1}{2\delta t}\left(\|\mathcal{E}^m\|^2 - \|\mathcal{E}^0\|^2\right) \\ &\leq -\frac{1}{2\delta t}\left(\|\nabla\mathcal{E}^m\|^2 - \|\nabla\mathcal{E}^0\|^2\right) - \sum_{n=1}^{m}\|\nabla\mathcal{E}^{n-\frac{1}{2}}\|^2 + \sum_{n=1}^{m}\|R^{n-\frac{1}{2}}\|\|\delta_t\mathcal{E}^{n-\frac{1}{2}} + \mathcal{E}^{n-\frac{1}{2}}\|\end{aligned}$$

Now application of Lemma 4 yields

$$\begin{aligned}&\frac{t_m^{1-\alpha}}{2\delta t\Gamma(2-\alpha)}\delta t\sum_{n=1}^{m}\|\delta_t\mathcal{E}^{n-\frac{1}{2}} + \mathcal{E}^{n-\frac{1}{2}}\|^2 + \frac{1}{2\delta t}\|\mathcal{E}^m\|^2 + \sum_{n=1}^{m}\|\mathcal{E}^{n-\frac{1}{2}}\|^2 \\ &+ \frac{1}{2\delta t}\|\nabla\mathcal{E}^m\|^2 + \sum_{n=1}^{m}\|\nabla\mathcal{E}^{n-\frac{1}{2}}\|^2 \\ &\leq \sum_{n=1}^{m}\|R^{n-\frac{1}{2}}\|\|\delta_t\mathcal{E}^{n-\frac{1}{2}} + \mathcal{E}^{n-\frac{1}{2}}\|.\end{aligned} \tag{2.27}$$

Using inequality $|xy| \leq \frac{1}{2\theta}x^2 + \frac{\theta}{2}y^2$, together with $\theta = \frac{t_m^{1-\alpha}}{\Gamma(2-\alpha)}$, we have

$$\begin{aligned}&\sum_{n=1}^{m}\|R^{n-\frac{1}{2}}\|\|\delta_t\mathcal{E}^{n-\frac{1}{2}} + \mathcal{E}^{n-\frac{1}{2}}\| \\ &\leq \frac{\Gamma(2-\alpha)}{2t_m^{1-\alpha}}\sum_{n=1}^{m}\|R^{n-\frac{1}{2}}\|^2 + \frac{t_m^{1-\alpha}}{2\Gamma(2-\alpha)}\sum_{n=1}^{m}\|\delta_t\mathcal{E}^{n-\frac{1}{2}} + \mathcal{E}^{n-\frac{1}{2}}\|^2.\end{aligned}$$

Using the above relation into Eq. (2.27), we have

$$\begin{aligned}&\frac{t_m^{1-\alpha}}{2\Gamma(2-\alpha)}\sum_{n=1}^{m}\|\delta_t\mathcal{E}^{n-\frac{1}{2}} + \mathcal{E}^{n-\frac{1}{2}}\|^2 + \frac{1}{2\delta t}\|\mathcal{E}^m\|^2 + \sum_{n=1}^{m}\|\mathcal{E}^{n-\frac{1}{2}}\|^2 \\ &+ \frac{1}{2\delta t}\|\nabla\mathcal{E}^m\|^2 + \sum_{n=1}^{m}\|\nabla\mathcal{E}^{n-\frac{1}{2}}\|^2 \\ &\leq \frac{\Gamma(2-\alpha)}{2t_m^{1-\alpha}}\sum_{n=1}^{m}\|R^{n-\frac{1}{2}}\|^2 + \frac{t_m^{1-\alpha}}{2\Gamma(2-\alpha)}\sum_{n=1}^{m}\|\delta_t\mathcal{E}^{n-\frac{1}{2}} + \mathcal{E}^{n-\frac{1}{2}}\|^2.\end{aligned} \tag{2.28}$$

Multiplying both sides of the above inequality by $2\delta t$ and switching index from m to n, with some calculation we get

$$\begin{aligned}
&\|\mathcal{E}^n\|^2 + 2\delta t \sum_{k=1}^{n} \|\mathcal{E}^{k-\frac{1}{2}}\|^2 + \|\nabla \mathcal{E}^n\|^2 \\
&\quad + 2\delta t \sum_{k=1}^{n} \|\nabla \mathcal{E}^{k-\frac{1}{2}}\|^2 \le \delta t \Gamma(2-\alpha) t_n^{\alpha-1} \sum_{j=1}^{n} \|R^{j-\frac{1}{2}}\|^2 \\
&\quad \le n\delta t \Gamma(2-\alpha) t_n^{\alpha-1} \max_{1\le j\le n} \|R^{j-\frac{1}{2}}\|^2 \\
&\|\mathcal{E}^n\|^2 \le n\delta t \Gamma(2-\alpha) t_n^{\alpha-1} \max_{1\le j\le n} \|R^{j-\frac{1}{2}}\|^2 \\
&\quad \le T^2 \Gamma(2-\alpha) C^2 \left(\delta t^{3-\alpha}\right)^2
\end{aligned}$$

Therefore, we have

$$\|\mathcal{E}^n\| \le C^* \delta t^{3-\alpha},$$

where $C^* = \sqrt{T^2\Gamma(2-\alpha)C^2}$, which completes the proof. □

3 The local collocation method for Spatial discretization

The local collocation method has been developed by taking the global domain Ω that contains the M discretization points. For each discretization point $\mathbf{x}_i$, $i = 1, 2, \dots, M$, there is a local sub-domain $\Omega_i = \{\mathbf{x}_j\}_{j=1}^{m_i}$, where m_i are the closest points of the discretized point $\mathbf{x}_i$ in sub-domain Ω_i. In the local interpolation form, the $u(\mathbf{x}, t_n)$ can be numerically approximated as

$$\hat{u}(\mathbf{x}, t_n) = \sum_{j=1}^{m_i} \lambda_j \phi(\|\mathbf{x} - \mathbf{x}_j\|) + \sum_{j=1}^{l} \gamma_j p_j(\mathbf{x}), \tag{3.1}$$

where $\{\lambda_j\}$ and $\{\gamma_j\}$ are coefficients at nth time level that need to be determined, ϕ is any considered radial basis function, considered norm is defined in Euclidean sense and $\{p_j(x)\}_{j=1}^{l}$ is the basis of the l-dimensional polynomial space of total degree $\le m-1$. The application of the interpolation condition on each sub-domain Ω_i give us

$$\hat{u}(\mathbf{x}_i, t_n) = u(\mathbf{x}_i, t_n),\ i = 1, 2, \dots, m_i, \tag{3.2}$$

with l homogeneous conditions

$$\sum_{j=1}^{m_i} \lambda_j p_k(\mathbf{x}_j) = 0,\ k = 1, 2, \dots, l. \tag{3.3}$$

Equations (3.2–3.3) can be written in the matrix form as

$$\begin{bmatrix} \Phi & P \\ P^t & O \end{bmatrix} \begin{bmatrix} \lambda \\ \gamma \end{bmatrix} = \begin{bmatrix} u^n\,|_{\Omega_i} \\ O \end{bmatrix} \tag{3.4}$$

where $\Phi := [\phi\|\mathbf{x}_j - \mathbf{x}_k\|]_{1\le j,k\le m_i}$, $P := [p_k(\mathbf{x}_j)]_{1\le j\le m_i, 1\le k\le l}$. The system (3.4) can be rewritten as

$$\Lambda_{\Omega_i} = A_{\Omega_i}^{-1} U_{\Omega_i}^n, \tag{3.5}$$

where $\Lambda_{\Omega_i} = [\lambda_1, \dots, \lambda_{m_i}, \gamma_1, \dots, \gamma_l]^\intercal$, $U_{\Omega_i}^n = [u(\mathbf{x}_1, t_n), \dots, u(\mathbf{x}_{m_i}, t_n), 0, \dots, 0]^\intercal$, and A_{Ω_i} is coefficient matrix defined in (3.4). At each stencil $\mathbf{x}_i \in \Omega_i$, we have approximation for $\mathscr{D}u(\mathbf{x}, t_n)$ as;

$$\begin{aligned}
\mathscr{D}\hat{u}(\mathbf{x}_i, t_n) &= \sum_{j=1}^{m_i} \lambda_j \mathscr{D}\phi(\|\mathbf{x}_i - \mathbf{x}_j\|) + \sum_{j=1}^{l} \gamma_j \mathscr{D}p_j(\mathbf{x}_i), \\
&= [\mathscr{D}\phi(\|\mathbf{x}_i - \mathbf{x}_1\|), \dots, \mathscr{D}\phi(\|\mathbf{x}_i - \mathbf{x}_{m_i}\|), \\
&\quad \mathscr{D}p_1(\mathbf{x}_i), \dots \mathscr{D}p_l(\mathbf{x}_i)]\Lambda_{\Omega_i} \\
&= \mathscr{D}\Psi_{\Omega_i} A_{\Omega_i}^{-1} U_{\Omega_i}^n,
\end{aligned} \tag{3.6}$$

where $\Psi_{\Omega_i} = [\phi(\|\mathbf{x}_i - \mathbf{x}_1\|), \dots, \phi(\|\mathbf{x}_i - \mathbf{x}_{m_i}\|), p_1(\mathbf{x}_i), \dots p_l(\mathbf{x}_i)]$. For each i, the local operator $\mathscr{D}\Psi_{\Omega_i} A_{\Omega_i}^{-1}$ is a $1 \times m_i$ row vector. For the application of the local collocation method as defined in (3.6), for each collocation point $\mathbf{x}_i \in \Omega$, to the linear operator $\mathscr{L}$ as defined in Eq. (2.20), we have

$$\mathscr{L}\Psi_{\Omega_i} A_{\Omega_i}^{-1} U_{\Omega_i}^n = F_i, \mathbf{x}_i \in \Omega \tag{3.7}$$

For each row we have only m_i nonzero entry that will be stored in M^2 global coefficient matrix, and extra spaces will be filled by zeros. Then, we get the following linear system

$$\mathbf{L}\mathbf{U}^n = \mathbf{F}. \tag{3.8}$$

The resulting system is sparse because in each row we have only m_i nonzero entries that can be calculated very efficiently and easily.

4 Numerical simulation and discussion

In this section, we present some numerical results for confirmation of the validity and efficiency of the present numerical method. To measure the accuracy of the method, we used maximum absolute error L_∞ and root mean square error L_{rms} which are defined by using the definition

$$\begin{aligned}
L_{\text{rms}} &= \sqrt{\frac{1}{M}\sum_{i=1}^{M} |u(x_i, T) - U(x_i, T)|^2}, \\
L_\infty &= \max_{1\le i\le M} |u(x_i, T) - U(x_i, T)|,
\end{aligned}$$

where M denotes the number of collocation points and $u(x_i, T)$ and $U(x_i, T)$ represent an exact and numerical solution of the considered problem. We calculated the convergence rate of the proposed method by using the formula $\frac{\log(E_1/E_2)}{\log(\delta t_1/\delta t_2)}$ where E_1 and E_2 are errors corresponding to temporal mesh size δt_1 and δt_2, respectively. To avoid the effect of the shape parameter ϵ over the numerical solution, the thin plate spline $r^4 \ln(r)$ RBF is used for computation purpose. In all sub-domain, the number of collocation points is constant.

Example 1 Consider the following one-dimensional test problem

$$ {}_0^c\mathscr{D}_t^{\alpha} u(x,t) + {}_0^c\mathscr{D}_t^{\alpha-1} u(x,t) + u(x,t) = \Delta u(x,t) + f(x,t). $$

The initial conditions and boundary conditions are calculated using analytic solution

$$ u(x,t) = t^3 (\sin x)^2. $$

The linear source term read $f(x,t) = \left(\frac{6t^{3-\alpha}}{\Gamma(4-\alpha)} + \frac{6t^{4-\alpha}}{\Gamma(5-\alpha)}\right)(\sin x)^2 - 2t^3 \cos 2x + t^3(\sin x)^2$.

Considered problem is solved with the present method for different values of α and δt on computational domain [0, 1]. The values of the root mean square error and absolute error for $M = 501$ spatial points, $m = 3$ at $T = 1$s are reported in Table 1. From the data given in Table 1, we can easily observe that the numerical rate has a good agreement with theoretical rate of convergence, i.e., $O(\delta t^{3-\alpha})$. The graph of numerical solution and absolute error in the numerical solution for $\alpha = 1.5$ and $N = 640$ is plotted in Fig. 1.

The values of different errors for $M = 1000$, $N = 1000$, $\alpha = 1.9$ and different values of local points m at $T = 1$ s are reported in Table 2. From the table, we observed that in most cases the improvement in the error is very small with respect to a increase in the number of local collocation points, while the computational time increases as m gets larger.

Example 2 Now consider the following one-dimensional test problem

$$ {}_0^c\mathscr{D}_t^{\alpha} u(x,t) + {}_0^c\mathscr{D}_t^{\alpha-1} u(x,t) + u(x,t) = \Delta u(x,t) + f(x,t). $$

The linear source term $f(x, t)$ along with initial conditions and boundary conditions is calculated using analytic solution

$$ u(x,t) = x\cos(x^2 + t^2). $$

It is not easy to find out the linear source term explicitly. Therefore, we used MATLAB symbolic calculation procedure for the same. We adopted this test problem from Hosseini et al. [25]; they solved the considered problem using RBF-based collocation method on the computational domain [0, 1]. The proposed method is compared with Hosseini et al. [25] at $T = 1.0$ s, and the results are given in Table 3. From Table 3, we can see that the present method gives better accuracy than [25]. Finally, the graph of numerical approximation and absolute error for $\alpha = 1.5$, $M = 201$ spatial points, $m = 3$ local points and $N = 200$ is reported in Fig.2.

Example 3 In this example, we consider two-dimensional test problem

$$ {}_0^c\mathscr{D}_t^{\alpha} u(x,y,t) + {}_0^c\mathscr{D}_t^{\alpha-1} u(x,y,t) + u(x,y,t) = \Delta u(x,y,t) + f(x,y,t). $$

The initial conditions and boundary conditions are calculated using analytic solution

$$ u(x,y,t) = t^4 \sin(\pi x + \pi y). $$

The linear source term read $f(x,t) = \left(\frac{24t^{4-\alpha}}{\Gamma(5-\alpha)} + \frac{24t^{5-\alpha}}{\Gamma(6-\alpha)} + 2t^4\pi^2\right)\sin(\pi x + \pi y) + t^4 \sin(\pi x + \pi y)$.

In this example, we consider a rectangular domain $\Omega = [0,1] \times [0,1]$ with 2025 uniform points and 2060 non-uniform points as shown in Fig. 3. The computational errors with $m = 5$ uniform and non-uniform points in local domain at $T = 1.0$ s are listed in Table 4 and Table 5, respectively. This table ensures that the computational convergence order is close to the theoretical convergence order. The behavior of the numerical solution and absolute error for $\alpha = 1.5$ and $N = 160$ is plotted in Fig. 4 for uniform points and in Fig. 5 for non-uniform points.

Example 4 Finally, we consider the two-dimensional test problem

$$ {}_0^c\mathscr{D}_t^{\alpha} u(x,y,t) + {}_0^c\mathscr{D}_t^{\alpha-1} u(x,y,t) + u(x,y,t) = \Delta u(x,y,t) + f(x,y,t). $$

The initial conditions and boundary conditions are calculated using analytic solution

Table 1 The different errors along with cpu time for different values of δt and α for Example 1

	$\alpha = 1.5$			$\alpha = 1.9$			
δt	L_∞	L_{rms}	Rate	L_∞	L_{rms}	Rate	cpu (s)
1/10	2.3879e−03	1.6759e−03	–	1.3760e−02	9.8112e−03	–	0.206
1/20	8.6047e−04	6.0373e−04	1.47	6.5907e−03	4.7162e−03	1.06	0.199
1/40	3.0834e−04	2.1632e−04	1.48	3.1163e−03	2.2348e−03	1.08	0.267
1/80	1.1004e−04	7.7184e−05	1.49	1.4634e−03	1.0508e−03	1.09	0.477
1/160	3.9131e−05	2.7439e−05	1.50	6.8491e−04	4.9209e−04	1.09	0.898

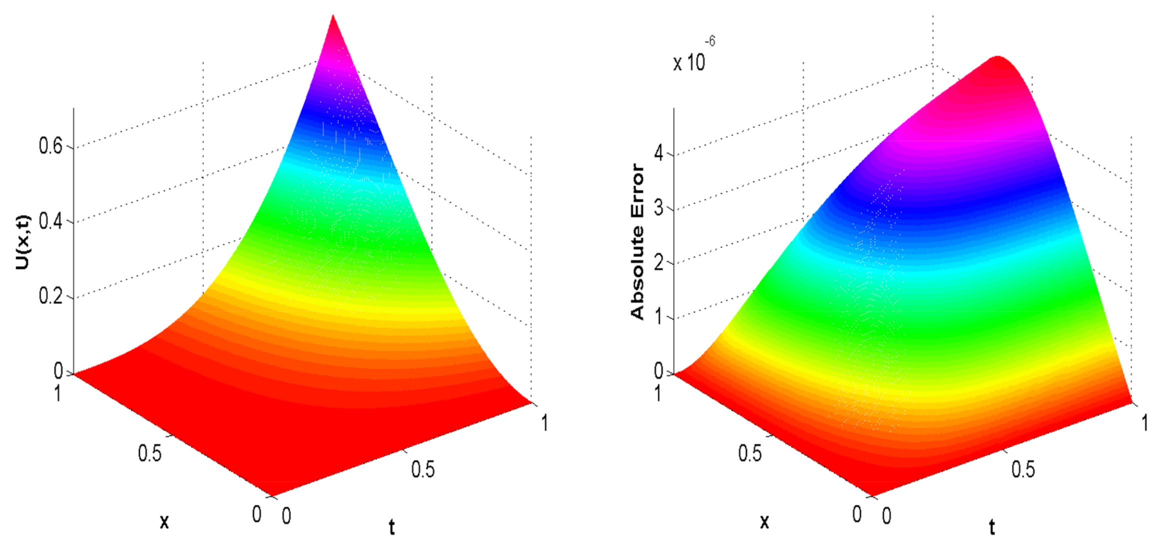

Fig. 1 Graph of numerical solution and absolute error with $\alpha = 1.5$ for Example 1

Table 2 The different errors along with cpu time for $\alpha = 1.9$ and different values of m for Example 1

m	L_∞	L_{rms}	cpu (s)
3	9.1474e−05	6.5786e−05	34.249
7	9.1472e−05	6.5785e−05	35.542
9	9.1494e−05	6.5804e−05	37.021
11	9.1483e−05	6.5794e−05	37.380
15	9.1484e−05	6.5796e−05	38.332

$u(x, y, t) = x^2 + y^2 + t^4.$

The linear source term read $f(x,t) = \frac{24t^{4-\alpha}}{\Gamma(5-\alpha)} + \frac{24t^{5-\alpha}}{\Gamma(6-\alpha)}$ $+(x^2 + y^2 + t^4) - 4.$

In this test problem, we consider four different complex-shape computational domains $\Omega_i, = 1, 2, 3, 4$ as shown in Fig. 6. The first one is circular domain as shown in the first part of Fig. 6 with center (0.5, 0.5) and radius $r = 0.5$. Table 6 shows errors on circular domain with $M = 2395$ spatial points, $m = 5$ at $T = 1.0$ s. Finally, Fig. 7 shows graph of numerical solution and also the graph of absolute error for $\alpha = 1.75$ and $N = 400$. After that, we consider irregular polar domain with uniform points as shown in the second part of Fig. 6 whose boundary is given by parametric equation $\{(r\cos\theta, r\sin\theta) : r = \frac{n+1}{3n^2}[n + 1 - \cos n\theta]\}$ with $n = 6$. The value of errors corresponding to L^∞ and RMS are listed in Table 7 with $M = 1982$ spatial points on irregular polar domain at $T = 1.0$ s. Figure 8 represents the graph of numerical approximation and also the graph of absolute error for $\alpha = 1.85$ and $N = 400$.

Next, in this test problem we consider a multi-connected domain which is designed by two circles which are non-concentric as shown in the third part of Fig. 6. The center and radius of internal circle and external circle are (0.7, 0.6), $r = 0.1$ and (0.5, 0.5), $r = 0.5$, respectively. We used Dirichlet boundary conditions for both the inner

Table 3 Comparison of the present method with method [25] for different values of α and δt for Example 2

		$\alpha = 1.25$		$\alpha = 1.5$		$\alpha = 1.75$		$\alpha = 1.95$	
M	δt	Present	Method [25]	Present	Method [25]	Present	Method [25]	Present	Method [25]
20									
	1/10	2.2600e−04	8.6205e−03	1.1434e−03	1.0377e−02	4.6511e−03	1.2172e−02	1.1609e−02	1.3240e−02
	1/30	1.1860e−04	3.7954e−03	2.5318e−04	5.3478e−03	1.3350e−03	6.4685e−03	4.1575e−03	5.3905e−03
	1/50	1.1289e−04	2.6038e−03	1.4989e−04	4.0987e−03	7.6143e−04	5.3163e−03	2.5658e−03	3.7930e−03
50									
	1/10	1.8197e−04	8.7725e−03	1.1427e−03	1.0560e−02	4.6361e−03	1.2388e−02	1.1618e−02	1.3476e- 02
	1/30	3.5426e−05	3.8668e−03	2.2873e−04	5.4453e−03	1.2702e−03	6.5897e−03	4.0390e−03	5.5036e−03
	1/50	2.2992e−05	2.6551e−03	1.0880e−04	4.1743e−03	6.8631e−04	5.4164e−03	2.4189e−03	3.8800e−03

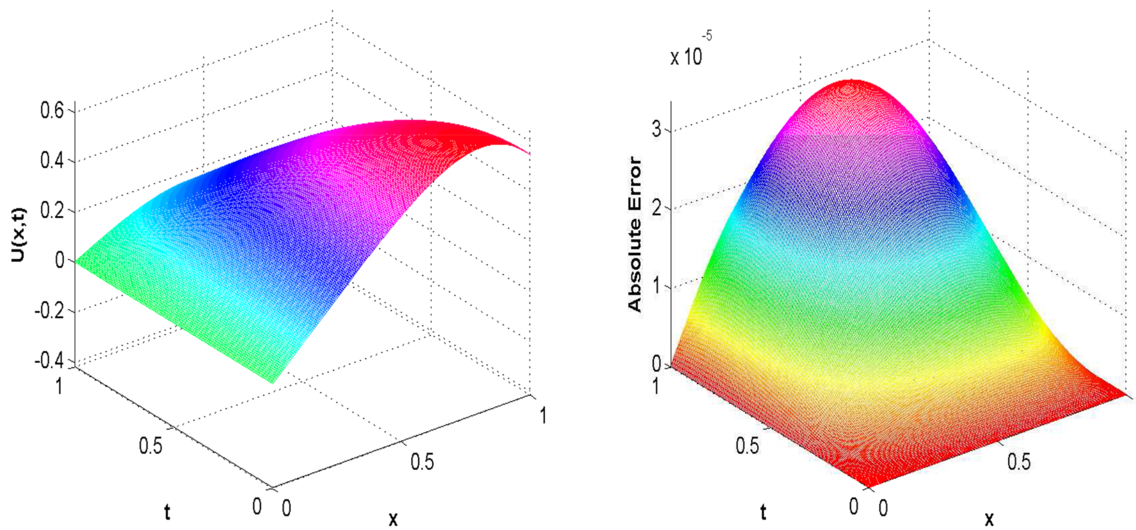

Fig. 2 Graph of numerical approximation of the solution and absolute error for Example 2

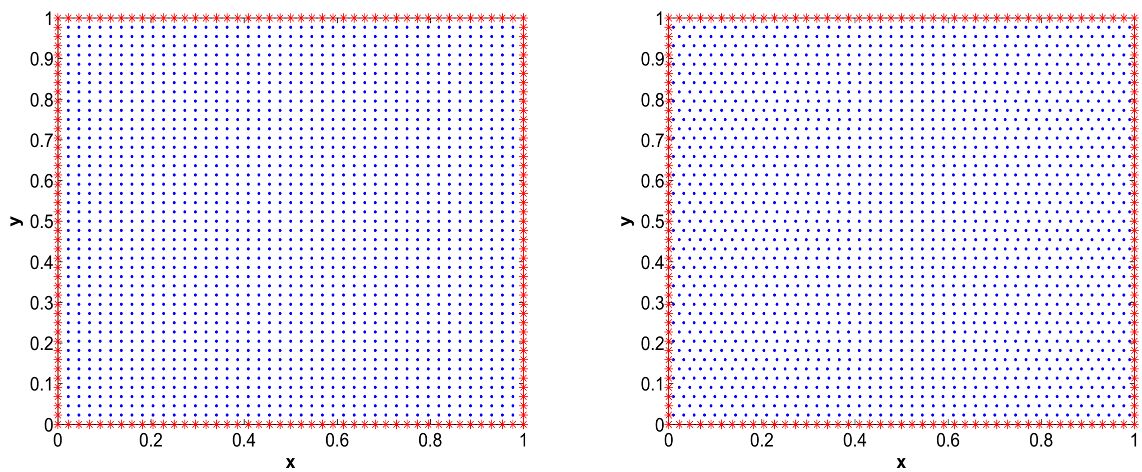

Fig. 3 Rectangular domain with uniform and non-uniform points for Example 3

Table 4 The value of errors and cpu time with $\alpha = 1.7, 1.9$ and different δt on rectangular domain with uniform points at time $T = 1.0$ s for Example 3

	$\alpha = 1.7$			$\alpha = 1.9$			
δt	L_∞	L_{rms}	Rate	L_∞	L_{rms}	Rate	cpu (s)
1/5	3.0420e−02	1.5017e−02	–	5.7458e−02	2.8347e−02	–	1.629
1/10	1.2917e−02	6.3781e−03	1.23	2.7619e−02	1.3636e−02	1.05	1.751
1/20	5.4532e−03	2.6931e−03	1.24	1.3079e−02	6.4626e−03	1.07	2.210
1/40	2.3351e−03	1.1537e−03	1.22	6.1953e−03	3.0631e−03	1.08	3.062

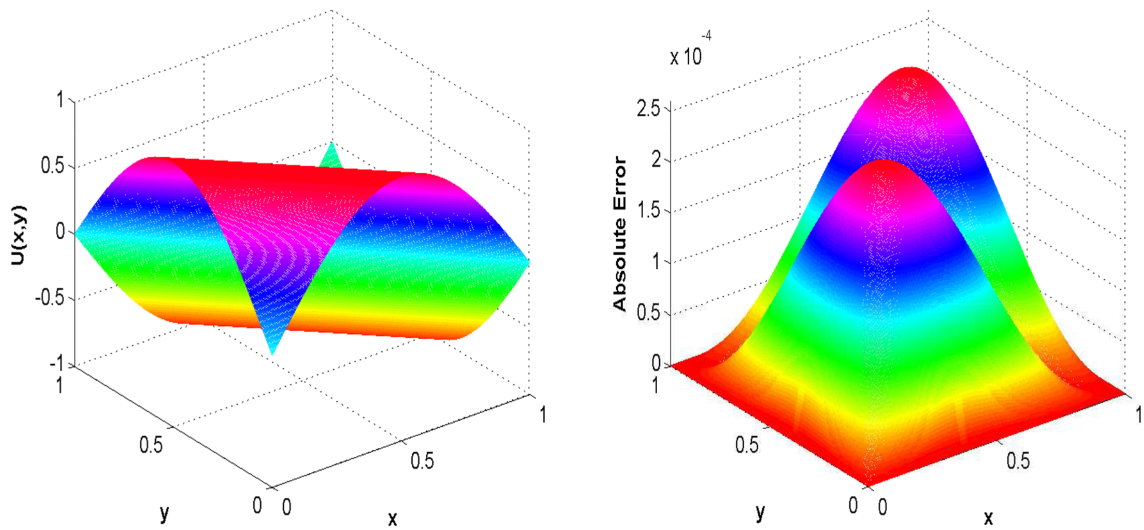

Fig. 4 Graph of numerical solution and absolute error on rectangular domain with uniform points for Example 3

Table 5 The value of errors and cpu time with $\alpha = 1.7, 1.9$ and for different δt on rectangular domain with non-uniform points at time $T = 1.0$ s for Example 3

	$\alpha = 1.7$			$\alpha = 1.9$			
δt	L_∞	L_{rms}	Rate	L_∞	L_{rms}	Rate	cpu (s)
1/5	3.0422e−02	1.4925e−02	–	5.7475e−02	2.8178e−02	–	5.027
1/10	1.2911e−02	6.3368e−03	1.24	2.7620e−02	1.3553e−02	1.06	1.757
1/20	5.4459e−03	2.6732e−03	1.25	1.3073e−02	6.4211e−03	1.08	2.734
1/40	2.3283e−03	1.1427e−03	1.23	6.1886e−03	3.0413e−03	1.08	3.002

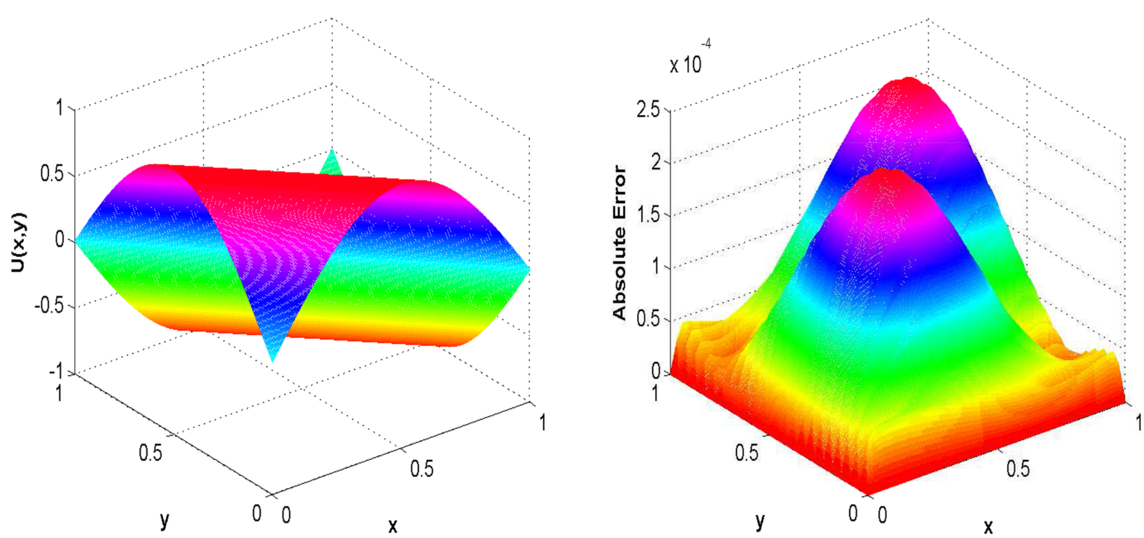

Fig. 5 Behavior of numerical solution and absolute error on the rectangular domain with non-uniform points for Example 3

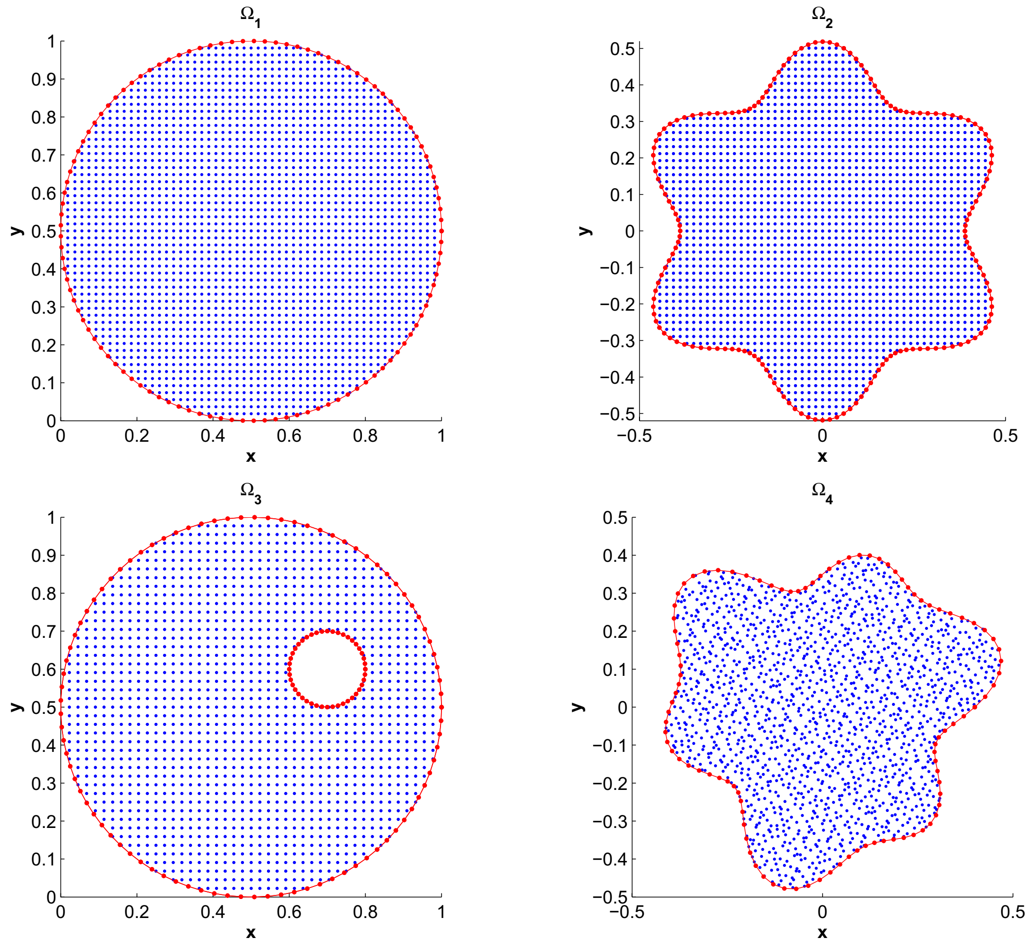

Fig. 6 The domains $\Omega_i, i = 1, 2, 3, 4$, for Example 4 with uniform and non-uniform points

Table 6 The value of both the errors and cpu time with $\alpha = 1.75, 1.95$ and for different δt on circular domain Ω_1 at time $T = 1.0$ s for Example 4

	$\alpha = 1.75$				$\alpha = 1.95$				
δt	L_∞	Rate	L_{rms}	Rate	L_∞	Rate	L_{rms}	Rate	cpu (s)
1/10	3.7326e−02	–	2.1307e−02	–	8.2147e−02	–	4.6734e−02	–	2.837
1/20	1.6016e−02	1.22	9.1336e−03	1.22	4.0930e−02	1.01	2.3258e−02	1.01	3.220
1/40	6.7931e−03	1.24	3.8663e−03	1.24	2.0093e−02	1.03	1.1409e−02	1.03	3.874
1/80	2.8569e−03	1.25	1.6185e−03	1.26	9.7731e−03	1.04	5.5439e−03	1.04	6.276
1/160	1.1887e−03	1.27	6.6630e−04	1.28	4.7237e−03	1.05	2.6748e−03	1.05	10.785
1/320	4.8466e−04	1.29	2.6532e−04	1.32	2.2690e−03	1.05	1.2800e−03	1.06	21.579

and outer circles. The errors are computed with $M = 1590$ spatial points at $T = 1.0$ s and reported in Table 8. From Table 8, we can easily see that the present method is very efficient and accurate. Finally, the graph of numerical solution and also the graph of absolute error on multi-connected domain for $\alpha = 1.95$ and $N = 1600$ are plotted in Fig. 9. Lastly, we consider irregular shape domain with boundary $\{r(\theta) = 0.4 + 0.05(\sin 6\theta + \sin 3\theta)\}$ and $M = 1645$ Halton non-uniform points as shown in the fourth part of Fig. 6. The numerical results on these non-uniform Halton points at $T = 1.0$ s are given in Table 9. The graph of numerical approximation and absolute error on domain Ω_4 for $N = 400$ and $\alpha = 1.55$ is given in Fig. 10.

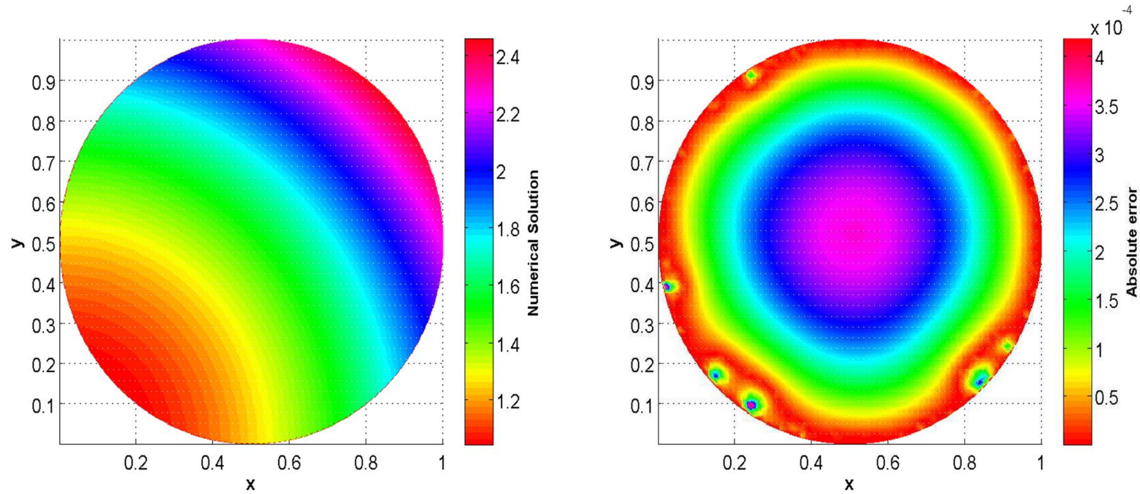

Fig. 7 Graph of approximated solution and absolute error on circular domain Ω_1 for Example 4

Table 7 The numerical errors along with cpu time with $\alpha = 1.75, 1.95$ and for different δt on irregular polar domain Ω_2 at time $T = 1.0$ s for Example 4

	$\alpha = 1.75$				$\alpha = 1.95$				
δt	L_∞	Rate	L_{rms}	Rate	L_∞	Rate	L_{rms}	Rate	cpu (s)
1/10	2.8492e−02	–	1.5193e−02	–	6.2616e−02	–	3.3332e−02	–	1.955
1/20	1.2112e−02	1.23	6.4347e−03	1.24	3.0908e−02	1.02	1.6419e−02	1.02	2.119
1/40	5.0642e−03	1.25	2.6646e−03	1.27	1.5083e−02	1.04	3.8419e−03	1.04	2.742
1/80	2.0652e−03	1.29	1.0621e−03	1.32	3.5064e−03	1.05	1.8240e−03	1.06	4.488
1/160	7.9585e−04	1.37	3.9004e−04	1.44	1.6685e−03	1.06	8.4691e−04	1.07	8.062

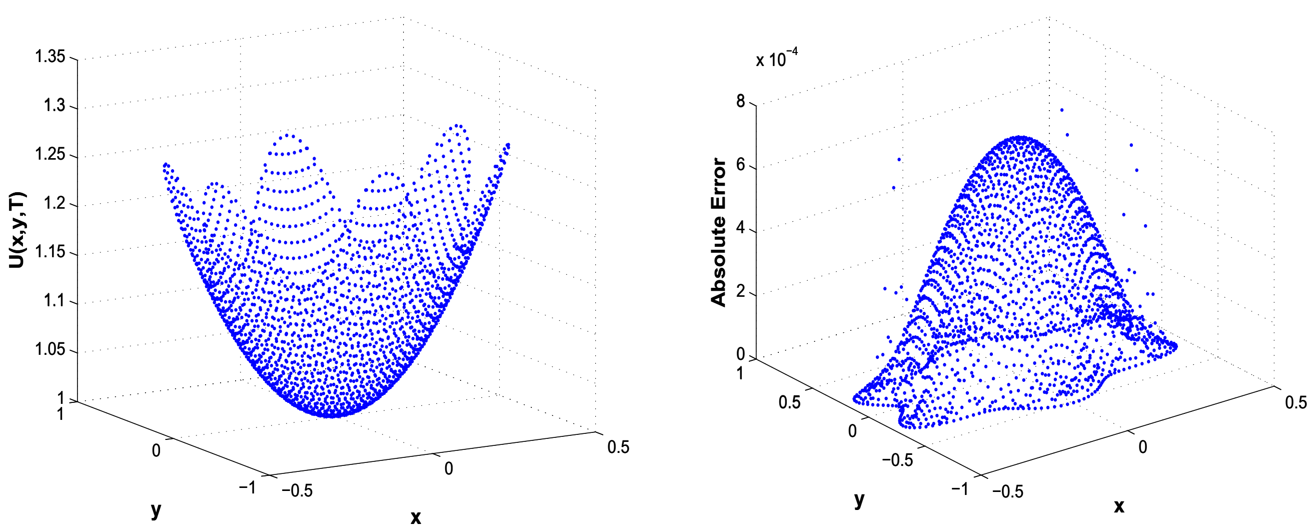

Fig. 8 Graph of numerical solution and absolute error on irregular polar domain Ω_2 for Example 4

Table 8 The computational errors along with cpu time with different values of α and δt on multi-connected domain Ω_3 at time $T = 1.0$ s for Example 4

	$\alpha = 1.55$			$\alpha = 1.95$			
δt	L_∞	L_{rms}	Rate	L_∞	L_{rms}	Rate	cpu (s)
1/25	3.0944e−03	1.6058e−03	–	2.1654e−02	1.1189e−02	–	2.026
1/50	1.1475e−03	5.9548e−04	1.431	1.0527e−02	5.4425e−03	1.040	2.653
1/100	4.2347e−04	2.1975e−04	1.438	5.1005e−03	2.6381e−03	1.045	4.239
1/200	1.5581e−04	8.0852e−05	1.442	2.4673e−03	1.2765e−03	1.047	7.388
1/400	5.7223e−05	2.9694e−05	1.445	1.1926e−03	6.1710e−04	1.048	16.726

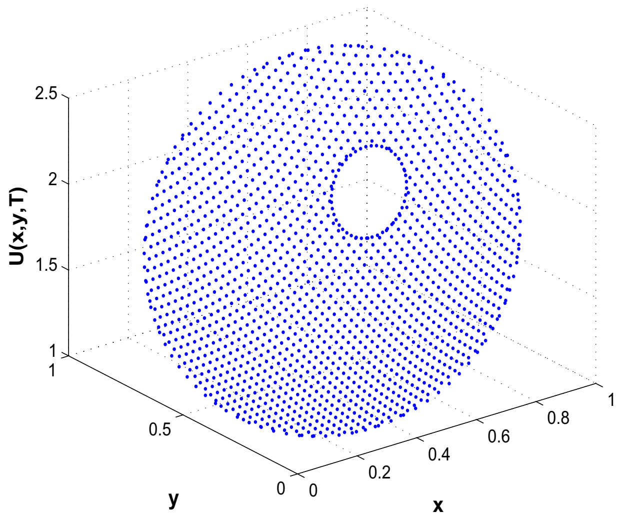

Fig. 9 Graph of approximated solution and absolute error on multi-connected domain Ω_3 for Example 4

Table 9 The value of both the errors and cpu time with $\alpha = 1.55, 1.95$ and for different δt on irregular polar domain with non-uniform Halton points Ω_4 at time $T = 1.0$ s for Example 4

	$\alpha = 1.55$			$\alpha = 1.95$			
δt	L_∞	L_{rms}	Rate	L_∞	L_{rms}	Rate	cpu (s)
1/25	2.7111e−03	1.4611e−03	–	1.8551e−02	9.9857e−03	–	1.890
1/50	1.0054e−03	5.4182e−04	1.431	8.9889e−03	4.8383e−03	1.045	2.714
1/100	3.7103e−04	1.9994e−04	1.438	4.3483e−03	2.3400e−03	1.047	4.139
1/200	1.3651e−04	7.3565e−05	1.442	2.1019e−03	1.1309e−03	1.048	7.049
1/400	5.0135e−05	2.7018e−05	1.445	1.0156e−03	5.4637e−04	1.049	16.272

5 Conclusion

In the present work, we have developed a local meshless method based on RBF for solving the time-fractional telegraph equation with the fractional derivative as defined in the Caputo sense. The time semi-discretization was done by finite difference method to obtain the semi-discrete scheme, and spatial discretization was done by RBF-based meshless method to obtain a fully discrete scheme. With the help of numerical examples, we shows that the computational convergence order in time is nicely close to theoretical order. To examine the efficiency of the proposed method, being suitable for irregular domain a numerical experiment on several complex domain was carried out. It was found that the method is robust and very pleasant to deal with regular as well as irregular domains.

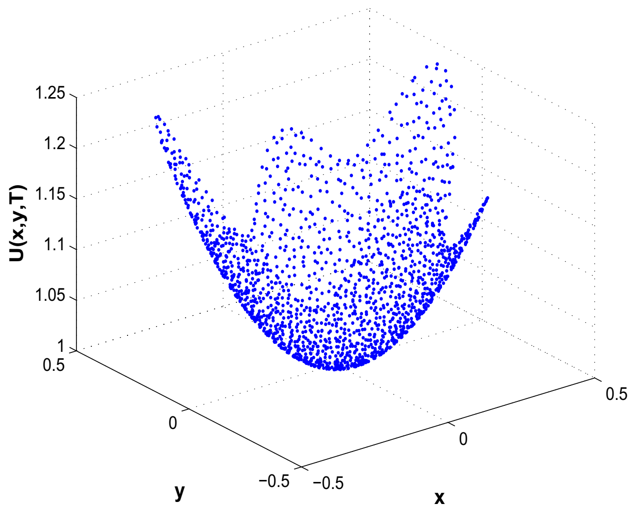

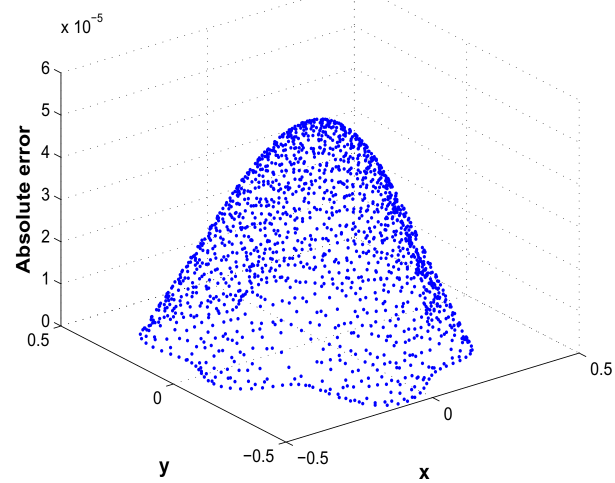

Fig. 10 Graph of approximated solution along with absolute error on domain Ω_4 for Example 4

Acknowledgements We would like to thank reviewers for their valuable comments and suggestions that really improved the quality of the paper.

Compliance with ethical standards

Conflict of interest The authors declare that there is no conflict of interests regarding the publication of this article.

References

1. Abbaszadeh M, Dehghan M (2017) An improved meshless method for solving two-dimensional distributed order time-fractional diffusion-wave equation with error estimate. Numer Algorithms 75(1):173–211
2. Bagley RL, Torvik PJ (1983) A theoretical basis for the application of fractional calculus to viscoelasticity. J Rheol 27(3):201–210
3. Banasiak J, Mika JR (1998) Singularly perturbed telegraph equations with applications in the random walk theory. Int J Stoch Anal 11(1):9–28
4. Cen Z, Huang J, Aimin X, Le A (2018) Numerical approximation of a time-fractional Black-Scholes equation. Comput Math Appl 75(8):2874–2887
5. Chen J, Liu F, Anh V (2008) Analytical solution for the time-fractional telegraph equation by the method of separating variables. J Math Anal Appl 338(2):1364–1377
6. Chen W, Ye L, Sun H (2010) Fractional diffusion equations by the Kansa method. Comput Math Appl 59(5):1614–1620
7. Das S, Vishal K, Gupta PK, Yildirim A (2011) An approximate analytical solution of time-fractional telegraph equation. Appl Math Comput 217(18):7405–7411
8. De Staelen RH, Hendy AS (2017) Numerically pricing double barrier options in a time-fractional black–scholes model. Comput Math Appl 74(6):1166–1175
9. Dehghan M, Abbaszadeh M (2017) A finite element method for the numerical solution of Rayleigh-Stokes problem for a heated generalized second grade fluid with fractional derivatives. Eng Comput 33(3):587–605
10. Dehghan M, Abbaszadeh M (2018) A finite difference/finite element technique with error estimate for space fractional tempered diffusion-wave equation. Comput Math Appl 75(8):2903–2914
11. Dehghan M, Abbaszadeh M, Mohebbi A (2015) Error estimate for the numerical solution of fractional reaction-subdiffusion process based on a meshless method. J Comput Appl Math 280:14–36
12. Dehghan M, Abbaszadeh M, Mohebbi A (2015) An implicit rbf meshless approach for solving the time fractional nonlinear sine-gordon and klein-gordon equations. Eng Anal Bound Elem 50:412–434
13. Dehghan M, Abbaszadeh M, Mohebbi A (2016) Analysis of a meshless method for the time fractional diffusion-wave equation. Numer Algorithms 73(2):445–476
14. Dehghan M, Ghesmati A (2010) Combination of meshless local weak and strong (mlws) forms to solve the two dimensional hyperbolic telegraph equation. Eng Anal Bound Elem 34(4):324–336
15. Dehghan M, Mohammadi V (2015) The numerical solution of cahn-hilliard (ch) equation in one, two and three-dimensions via globally radial basis functions (grbfs) and rbfs-differential quadrature (rbfs-dq) methods. Eng Anal Bound Elem 51:74–100
16. Dehghan M, Shokri A (2008) A numerical method for solving the hyperbolic telegraph equation. Numer Methods Part Differ Equ Int J 24(4):1080–1093
17. Dehghan M, Yousefi SA, Lotfi A (2011) The use of he's variational iteration method for solving the telegraph and fractional telegraph equations. Int J Numer Methods Biomed Eng 27(2):219–231
18. Esen A, Bulut F, Oruç Ö (2016) A unified approach for the numerical solution of time fractional burgers' type equations. Eur Phys J Plus 131(4):116
19. Ghandehari MAM, Ranjbar M (2013) A numerical method for solving a fractional partial differential equation through converting it into an nlp problem. Comput Math Appl 65(7):975–982
20. Ghehsareh HR, Bateni SH, Zaghian A (2015) A meshfree method based on the radial basis functions for solution of two-dimensional fractional evolution equation. Eng Anal Bound Elem 61:52–60
21. Ghehsareh HR, Raei M, Zaghian A (2019) Application of meshless local petrov–galerkin technique to simulate two-dimensional time-fractional tricomi-type problem. J Braz Soc Mech Sci Eng 41(6):252
22. Ghehsareh HR, Zaghian A, Raei M (2018) A local weak form meshless method to simulate a variable order time-fractional mobile–immobile transport model. Eng Anal Bound Elem 90:63–75
23. Ghehsareh HR, Zaghian A, Zabetzadeh SM (2019) An efficient meshless computational technique to simulate nonlinear anomalous reaction-diffusion process in two-dimensional space. Nonlinear Dyn 96(2):1191–1211

24. Gorenflo R, Mainardi F, Scalas E, Raberto M (2001) Fractional calculus and continuous-time finance iii: the diffusion limit. In: Kohlmann M, Tang S (eds) Mathematical finance. Springer, Berlin, pp 171–180
25. Hosseini VR, Chen W, Avazzadeh Z (2014) Numerical solution of fractional telegraph equation by using radial basis functions. Eng Analy Bound Elem 38:31–39
26. Hosseini VR, Shivanian E, Chen W (2015) Local integration of 2-d fractional telegraph equation via local radial point interpolant approximation. Eur Phys J Plus 130(2):33
27. Hosseini VR, Shivanian E, Chen W (2016) Local radial point interpolation (mlrpi) method for solving time fractional diffusion-wave equation with damping. J Comput Phys 312:307–332
28. Jiang W, Lin Y (2011) Representation of exact solution for the time-fractional telegraph equation in the reproducing kernel space. Commun Nonlinear Sci Numer Simul 16(9):3639–3645
29. Kumar A, Bhardwaj A (2020) A local meshless method for time fractional nonlinear diffusion wave equation. Numer Algorithms. https://doi.org/10.1007/s11075-019-00866-9
30. Kumar A, Bhardwaj A, Kumar BVR (2019) A meshless local collocation method for time fractional diffusion wave equation. Comput Math Appl 78(6):1851–1861
31. Kumar K, Pandey RK, Sharma S, Xu Y (2019) Numerical scheme with convergence for a generalized time-fractional telegraph-type equation. Numer Methods Part Differ Equ 35(3):1164–1183
32. Li C, Cao J (2012) A finite difference method for time-fractional telegraph equation. In: Mechatronics and Embedded Systems and Applications (MESA), 2012 IEEE/ASME International Conference on, pp 314–318. IEEE, 2012
33. Liang Y, Yao Z, Wang Z (2020) Fast high order difference schemes for the time fractional telegraph equation. Numer Methods Part Differ Equ 36(1):154–172
34. Liu J, Li X, Xiuling H (2019) A rbf-based differential quadrature method for solving two-dimensional variable-order time fractional advection-diffusion equation. J Comput Phys 384:222–238
35. Liu Q, Liu F, Turner I, Anh V, Gu YT (2014) A rbf meshless approach for modeling a fractal mobile/immobile transport model. Appl Math Comput 226:336–347
36. Mainardi F, Paradisi P (2001) Fractional diffusive waves. J Comput Acoust 9(04):1417–1436
37. Mittal RC, Bhatia R (2014) A numerical study of two dimensional hyperbolic telegraph equation by modified b-spline differential quadrature method. Appl Math Comput 244:976–997
38. Mohebbi A, Abbaszadeh M, Dehghan M (2014) The meshless method of radial basis functions for the numerical solution of time fractional telegraph equation. Int J Numer Methods Heat Fluid Flow 24(8):1636–1659
39. Momani S (2005) Analytic and approximate solutions of the space-and time-fractional telegraph equations. Appl Math Comput 170(2):1126–1134
40. Nikan O, Machado JAT, Golbabai A, Nikazad T (2019) Numerical investigation of the nonlinear modified anomalous diffusion process. Nonlinear Dyn 97(4):2757–2775
41. Oruç Ö (2018) A numerical procedure based on hermite wavelets for two-dimensional hyperbolic telegraph equation. Eng Comput 34(4):741–755
42. Oruç Ömer (2019) A meshfree computational approach based on multiple-scale pascal polynomials for numerical solution of a 2d elliptic problem with nonlocal boundary conditions. In: International journal of computational methods, p 1950080, 2019
43. Oruç Ö (2019) A meshless multiple-scale polynomial method for numerical solution of 3d convection–diffusion problems with variable coefficients. Eng Comput. https://doi.org/10.1007/s00366-019-00758-5
44. Oruç Ö (2019) Numerical solution to the deflection of thin plates using the two-dimensional Berger equation with a meshless method based on multiple-scale pascal polynomials. Appl Math Modell 74:441–456
45. Oruç Ö (2020) Two meshless methods based on local radial basis function and barycentric rational interpolation for solving 2D viscoelastic wave equation. Comput Math Appl. https://doi.org/10.1016/j.camwa.2020.01.025
46. Oruç Ö, Esen A, Bulut F (2019) A haar wavelet approximation for two-dimensional time fractional reaction-subdiffusion equation. Eng Comput 35(1):75–86
47. Ren J, Sun Z-Z, Zhao X (2013) Compact difference scheme for the fractional sub-diffusion equation with Neumann boundary conditions. J Comput Phys 232(1):456–467
48. Rudolf H (2000) Applications of fractional calculus in physics. World Scientific, Singapore
49. Salehi R (2017) A meshless point collocation method for 2-d multi-term time fractional diffusion-wave equation. Numer Algorithms 74(4):1145–1168
50. Sepehrian B, Shamohammadi Z (2018) Numerical solution of nonlinear time-fractional telegraph equation by radial basis function collocation method. Iranian J Sci Technol Trans A Sci 42(4):2091–2104
51. Shivanian E (2016) Spectral meshless radial point interpolation (smrpi) method to two-dimensional fractional telegraph equation. Math Methods Appl Sci 39(7):1820–1835
52. Shivanian E (2017) Analysis of the time fractional 2-d diffusion-wave equation via moving least square (mls) approximation. Int J Appl Comput Math 3(3):2447–2466
53. Shivanian E, Abbasbandy S, Alhuthali MS, Alsulami HH (2015) Local integration of 2-d fractional telegraph equation via moving least squares approximation. Eng Anal Bound Elem 56:98–105
54. Shivanian E, Jafarabadi A (2017) An improved spectral meshless radial point interpolation for a class of time-dependent fractional integral equations: 2d fractional evolution equation. J Comput Appl Math 325:18–33
55. Shivanian E, Jafarabadi A (2018) Capillary formation in tumor angiogenesis through meshless weak and strong local radial point interpolation. Eng Comput 34(3):603–619
56. Shivanian E, Khodabandehlo HR (2014) Meshless local radial point interpolation (mlrpi) on the telegraph equation with purely integral conditions. Eur Phys J Plus 129(11):241
57. HongGuang Sun, Zhang Y, Baleanu D, Chen W, Chen Y (2018) A new collection of real world applications of fractional calculus in science and engineering. Commun Nonlinear Sci Numer Simul 64:213–231
58. Sun Z, Xiaonan W (2006) A fully discrete difference scheme for a diffusion-wave system. Appl Numer Math 56(2):193–209
59. Vyawahare VA, Nataraj PSV (2013) Fractional-order modeling of neutron transport in a nuclear reactor. Appl Math Modell 37(23):9747–9767
60. Wang Y, Mei L (2017) Generalized finite difference/spectral galerkin approximations for the time-fractional telegraph equation. Adv Differ Equ 2017(1):281
61. Yıldırım A (2010) He's homotopy perturbation method for solving the space-and time-fractional telegraph equations. Int J Comput Math 87(13):2998–3006
62. Zhang Y, Sun Z, Zhao X (2012) Compact alternating direction implicit scheme for the two-dimensional fractional diffusion-wave equation. SIAM J Numer Anal 50(3):1535–1555
63. Zhao Z, Li C (2012) Fractional difference/finite element approximations for the time-space fractional telegraph equation. Appl Math Comput 219(6):2975–2988
64. Zhou F, Xiaoyong X (2017) Numerical solution of time-fractional diffusion-wave equations via Chebyshev wavelets collocation method. Adv Math Phys 2017:2610804

Publisher's Note Springer Nature remains neutral with regard to jurisdictional claims in published maps and institutional affiliations.